university of groningen

University Medical Center Groningen

University of Groningen

Determination of the number of psi ' events at BESIII

Ablikim, M.; Achasov, M. N.; Albayrak, O.; Ambrose, D. J.; An, F. F.; An, Q.; Bai, J. Z.; Ban, Y.; Becker, J.; Bennett, J. V.

Published in:
Chinese Physics C

DOI:
10.1088/1674-1137/37/6/063001

IMPORTANT NOTE: You are advised to consult the publisher's version (publisher's PDF) if you wish to cite from it. Please check the document version below.

Document Version
Publisher's PDF, also known as Version of record

Publication date:
2013

Link to publication in University of Groningen/UMCG research database

Citation for published version (APA):
Ablikim, M., Achasov, M. N., Albayrak, O., Ambrose, D. J., An, F. F., An, Q., Bai, J. Z., Ban, Y., Becker, J., Bennett, J. V., Berger, N., Bertani, M., Bian, J. M., Boger, E., Bondarenko, O., Boyko, I., Briere, R. A., Bytev, V., Cai, X., ... BESIII Collaboration (2013). Determination of the number of psi ' events at BESIII. *Chinese Physics C, 37*(6), Article 063001. https://doi.org/10.1088/1674-1137/37/6/063001

Copyright
Other than for strictly personal use, it is not permitted to download or to forward/distribute the text or part of it without the consent of the author(s) and/or copyright holder(s), unless the work is under an open content license (like Creative Commons).

The publication may also be distributed here under the terms of Article 25fa of the Dutch Copyright Act, indicated by the “Taverne” license. More information can be found on the University of Groningen website: https://www.rug.nl/library/open-access/self-archiving-pure/taverne-amendment.

Take-down policy
If you believe that this document breaches copyright please contact us providing details, and we will remove access to the work immediately and investigate your claim.

Downloaded from the University of Groningen/UMCG research database (Pure): http://www.rug.nl/research/portal. For technical reasons the number of authors shown on this cover page is limited to 10 maximum.

Download date: 12-03-2024

Chinese Physics C

PARTICLES AND FIELDS

Determination of the number of ψ' events at BESIII

To cite this article: M. Ablikim *et al* 2013 *Chinese Phys. C* **37** 063001

View the article online for updates and enhancements.

Related content

- Determination of the number of J/ events with J/ inclusive decays
  M. Ablikim, M. N. Achasov, D. J. Ambrose et al.
- Measurement of the integrated luminosities of the data taken by BESIII at s = 3.650 and 3.773 GeV
  M. Ablikim, M. N. Achasov, O. Albayrak et al.
- Observation of a pp mass threshold enhancement in + J/(J/ pp) decay
  M. Ablikim, M. N. Achasov, L. An et al.

Recent citations

- Study of J/ and (3686) decays to +
  M. Ablikim *et al*
- Search for (3686)c((1405))+0
  M. Ablikim *et al*
- Observation of c2 and c0,2
  M. Ablikim *et al*

This content was downloaded from IP address 129.125.148.244 on 26/04/2018 at 12:11

Determination of the number of ψ' events at BESIII*

M. Ablikim(麦迪娜)[1] M. N. Achasov[6] O. Albayrak[3] D. J. Ambrose[39] F. F. An(安芬芬)[1] Q. An(安琪)[40] J. Z. Bai(白景芝)[1] Y. Ban(班勇)[26] J. Becker[2] J. V. Bennett[16] N. Berger[1] M. Bertani[17A] J. M. Bian(边渐鸣)[38] E. Boger[19,a] O. Bondarenko[20] I. Boyko[19] R. A. Briere[3] V. Bytev[19] X. Cai(蔡啸)[1] O. Cakir[34A] A. Calcaterra[17A] G. F. Cao(曹国富)[1] S. A. Cetin[34B] J. F. Chang(常劲帆)[1] G. Chelkov[19,a] G. Chen(陈刚)[1] H. S. Chen(陈和生)[1] J. C. Chen(陈江川)[1] M. L. Chen(陈玛丽)[1] S. J. Chen(陈申见)[24] X. Chen(谌勋)[26] Y. B. Chen(陈元柏)[1] H. P. Cheng(程和平)[14] Y. P. Chu(初元萍)[1] D. Cronin-Hennessy[38] H. L. Dai(代洪亮)[1] J. P. Dai(代建平)[1] D. Dedovich[19] Z. Y. Deng(邓子艳)[1] A. Denig[18] I. Denysenko[19,b] M. Destefanis[43A,43C] W. M. Ding(丁伟民)[28] Y. Ding(丁勇)[22] L. Y. Dong(董燎原)[1] M. Y. Dong(董明义)[1] S. X. Du(杜书先)[46] J. Fang(方建)[1] S. S. Fang(房双世)[1] L. Fava[43B,43C] C. Q. Feng(封常青)[40] R. B. Ferroli[17A] P. Friedel[2] C. D. Fu(傅成栋)[1] Y. Gao(高原宁)[33] C. Geng(耿聪)[40] K. Goetzen[7] W. X. Gong(龚文煊)[1] W. Gradl[18] M. Greco[43A,43C] M. H. Gu(顾旻皓)[1] Y. T. Gu(顾运厅)[9] Y. H. Guan(管颖慧)[36] A. Q. Guo(郭爱强)[25] L. B. Guo(郭立波)[23] T. Guo(郭暾)[23] Y. P. Guo(郭玉萍)[25] Y. L. Han(韩艳良)[1] F. A. Harris[37] K. L. He(何康林)[1] M. He(何苗)[1] Z. Y. He(何振亚)[25] T. Held[2] Y. K. Heng(衡月昆)[1] Z. L. Hou(侯治龙)[1] C. Hu(胡琛)[23] H. M. Hu(胡海明)[1] J. F. Hu(胡继峰)[35] T. Hu(胡涛)[1] G. M. Huang(黄光明)[4] G. S. Huang(黄光顺)[40] J. S. Huang(黄金书)[12] L. Huang(黄亮)[1] X. T. Huang(黄性涛)[28] Y. Huang(黄勇)[24] Y. P. Huang(黄燕萍)[1] T. Hussain[42] C. S. Ji(姬长胜)[40] Q. Ji(纪全)[1] Q. P. Ji(姬清平)[25] X. B. Ji(季晓斌)[1] X. L. Ji(季筱璐)[1] L. L. Jiang(姜丽丽)[1] X. S. Jiang(江晓山)[1] J. B. Jiao(焦健斌)[28] Z. Jiao(焦铮)[14] D. P. Jin(金大鹏)[1] S. Jin(金山)[1] F. F. Jing(景繁凡)[33] N. Kalantar-Nayestanaki[20] M. Kavatsyuk[20] B. Kopf[2] M. Kornicer[37] W. Kuehn[35] W. Lai(赖蔚)[1] J. S. Lange[35] M. Leyhe[2] C. H. Li(李春花)[1] Cheng Li(李澄)[40] Cui Li(李翠)[40] D. M. Li(李德民)[46] F. Li(李飞)[1] G. Li(李刚)[1] H. B. Li(李海波)[1] J. C. Li(李家才)[1] K. Li(李康)[10] Lei Li(李蕾)[1] Q. J. Li(李秋菊)[1] S. L. Li(李绍莉)[1] W. D. Li(李卫东)[1] W. G. Li(李卫国)[1] X. L. Li(李晓玲)[28] X. N. Li(李小男)[1] X. Q. Li(李学潜)[25] X. R. Li(李秀荣)[27] Z. B. Li(李志兵)[32] H. Liang(梁昊)[40] Y. F. Liang(梁勇飞)[30] Y. T. Liang(梁羽铁)[35] G. R. Liao(廖广瑞)[33] X. T. Liao(廖小涛)[1] D. Lin(Lin)[11] B. J. Liu(刘北江)[1] C. L. Liu[3] C. X. Liu(刘春秀)[1] F. H. Liu(刘福虎)[29] Fang Liu(刘芳)[1] Feng Liu(刘峰)[4] H. Liu(刘虎)[1] H. B. Liu(刘宏邦)[9] H. H. Liu(刘汇慧)[13] H. M. Liu(刘怀民)[1] H. W. Liu(刘红薇)[1] J. P. Liu(刘觉平)[44] K. Liu(刘凯)[33] K. Y. Liu(刘魁勇)[22] Kai Liu(刘凯)[36] P. L. Liu(刘佩莲)[28] Q. Liu(刘倩)[36] S. B. Liu(刘树彬)[40] X. Liu(刘翔)[21] Y. B. Liu(刘玉斌)[25] Z. A. Liu(刘振安)[1] Zhiqiang Liu(刘志强)[1] Zhiqing Liu(刘智青)[1] H. Loehner[20] G. R. Lu(鲁公儒)[12] H. J. Lu(吕海江)[14] J. G. Lu(吕军光)[1] Q. W. Lu(吕绮雯)[29] X. R. Lu(吕晓睿)[36] Y. P. Lu(卢云鹏)[1] C. L. Luo(罗成林)[23] M. X. Luo(罗民兴)[45] T. Luo[37] X. L. Luo(罗小兰)[1] M. Lv(吕蒙)[1] C. L. Ma(马长利)[36] F. C. Ma(马凤才)[22] H. L. Ma(马海龙)[1] Q. M. Ma(马秋梅)[1] S. Ma(马斯)[1] T. Ma(马天)[1] X. Y. Ma(马骁妍)[1] F. E. Maas[11] M. Maggiora[43A,43C] Q. A. Malik[42] Y. J. Mao(冒亚军)[26] Z. P. Mao(毛泽普)[1] J. G. Messchendorp[20] J. Min(闵建)[1] T. J. Min(闵天觉)[1] R. E. Mitchell[16] X. H. Mo(莫晓虎)[1]

Received 29 September 2012, Revised 9 January 2013

*Supported by Ministry of Science and Technology of China (2009CB825200), National Natural Science Foundation of China (NSFC) (10625524, 10821063, 10825524, 10835001, 10935007, 11125525, 10975143, 10979058), Joint Funds of the National Natural Science Foundation of China (11079008, 11179007), Chinese Academy of Sciences (CAS) Large-Scale Scientific Facility Program; CAS (KJCX2-YW-N29, KJCX2-YW-N45), 100 Talents Program of CAS, Istituto Nazionale di Fisica Nucleare, Italy, Ministry of Development of Turkey (DPT2006K-120470), U. S. Department of Energy (DE-FG02-04ER41291, DE-FG02-91ER40682, DE-FG02-94ER40823), U.S. National Science Foundation, University of Groningen (RuG) and the Helmholtzzentrum fuer Schwerionenforschung GmbH (GSI), Darmstadt, WCU Program of National Research Foundation of Korea (R32-2008-000-10155-0)

©2013 Chinese Physical Society and the Institute of High Energy Physics of the Chinese Academy of Sciences and the Institute of Modern Physics of the Chinese Academy of Sciences and IOP Publishing Ltd

C. Morales Morales[11] N. Yu. Muchnoi[6] H. Muramatsu[39] Y. Nefedov[19] C. Nicholson(宁洁)[36] I. B. Nikolaev[6]
Z. Ning(宁哲)[1] S. L. Olsen(馬鵬)[27] Q. Ouyang(欧阳群)[1] S. Pacetti[17B] J. W. Park(卞正烷)[27] M. Pelizaeus[2]
H. P. Peng(彭海平)[40] K. Peters[7] J. L. Ping(平加伦)[23] R. G. Ping(平荣刚)[1] R. Poling[38] E. Prencipe[18]
M. Qi(祁鸣)[24] S. Qian(钱森)[1] C. F. Qiao(乔从丰)[36] L. Q. Qin(秦丽清)[28] X. S. Qin(秦小帅)[1] Y. Qin(秦瑶)[26]
Z. H. Qin(秦中华)[1] J. F. Qiu(邱进发)[1] K. H. Rashid[42] G. Rong(荣刚)[1] X. D. Ruan(阮向东)[9]
A. Sarantsev[19,c] B. D. Schaefer[16] M. Shao(邵明)[40] C. P. Shen[37,d] X. Y. Shen(沈肖雁)[1] H. Y. Sheng(盛华义)[1]
M. R. Shepherd[16] X. Y. Song(宋新颖)[1] S. Spataro[43A,43C] B. Spruck[35] D. H. Sun(孙德辉)[1]
G. X. Sun(孙功星)[1] J. F. Sun(孙俊峰)[12] S. S. Sun(孙胜森)[1] Y. J. Sun(孙勇杰)[40] Y. Z. Sun(孙永昭)[1]
Z. J. Sun(孙志嘉)[1] Z. T. Sun(孙振田)[40] C. J. Tang(唐昌建)[30] X. Tang(唐晓)[1] I. Tapan[34C] E. H. Thorndike[39]
D. Toth[38] M. Ullrich[35] G. S. Varner[37] B. Q. Wang(王博群)[26] D. Wang(王东)[26] D. Y. Wang(王大勇)[26]
K. Wang(王科)[1] L. L. Wang(王亮亮)[1] L. S. Wang(王灵淑)[1] M. Wang(王萌)[28] P. Wang(王平)[1]
P. L. Wang(王佩良)[1] Q. J. Wang(王庆娟)[1] S. G. Wang(王思广)[26] X. F. Wang(王雄飞)[33] X. L. Wang(汪晓莲)[40]
Y. F. Wang(王贻芳)[1] Z. Wang(王铮)[1] Z. G. Wang(王志刚)[1] Z. Y. Wang(王至勇)[1] D. H. Wei(魏代会)[8]
J. B. Wei(韦江波)[26] P. Weidenkaff[18] Q. G. Wen(文群刚)[40] S. P. Wen(文硕频)[1] M. Werner[35] U. Wiedner[2]
L. H. Wu(伍灵慧)[1] N. Wu(吴宁)[1] S. X. Wu(吴硕星)[40] W. Wu(吴蔚)[25] Z. Wu(吴智)[1] L. G. Xia(夏力钢)[33]
Y. X Xia(夏宇)[15] Z. J. Xiao(肖振军)[23] Y. G. Xie(谢宇广)[1] Q. L. Xiu(修青磊)[1] G. F. Xu(许国发)[1]
G. M. Xu(徐光明)[26] Q. J. Xu(徐庆君)[10] Q. N. Xu(徐庆年)[36] X. P. Xu(徐新平)[31] Z. R. Xu(许志蕊)[40]
F. Xue(薛飞)[4] Z. Xue(薛镇)[1] L. Yan(严亮)[40] W. B. Yan(鄢文标)[40] Y. H. Yan(颜永红)[15] H. X. Yang(杨洪勋)[1]
Y. Yang(杨迎)[4] Y. X. Yang(杨永栩)[8] H. Ye(叶桦)[1] M. Ye(叶梅)[1] M. H. Ye(叶铭汉)[5] B. X. Yu(俞伯祥)[1]
C. X. Yu(喻纯旭)[25] H. W. Yu(于海旺)[26] J. S. Yu(俞洁晟)[21] S. P. Yu(于帅鹏)[28] C. Z. Yuan(苑长征)[1]
Y. Yuan(袁野)[1] A. A. Zafar[42] A. Zallo[17A] Y. Zeng(曾云)[15] B. X. Zhang(张丙新)[1] B. Y. Zhang(张炳云)[1]
C. Zhang(张驰)[24] C. C. Zhang(张长春)[1] D. H. Zhang(张达华)[1] H. H. Zhang(张宏浩)[32] H. Y. Zhang(章红宇)[1]
J. Q. Zhang(张敬庆)[1] J. W. Zhang(张家文)[1] J. Y. Zhang(张建勇)[1] J. Z. Zhang(张景芝)[1] LiLi Zhang(张丽丽)[15]
R. Zhang(张瑞)[36] S. H. Zhang(张书华)[1] X. J. Zhang(张晓杰)[1] X. Y. Zhang(张学尧)[28] Y. Zhang(张瑶)[1]
Y. H. Zhang(张银鸿)[1] Z. P. Zhang(张子平)[40] Z. Y. Zhang(张振宇)[44] Zhenghao Zhang(张正好)[4] G. Zhao(赵光)[1]
H. S. Zhao(赵海升)[1] J. W. Zhao(赵京伟)[1] K. X. Zhao(赵凯旋)[23] Lei Zhao(赵雷)[40] Ling Zhao(赵玲)[1]
M. G. Zhao(赵明刚)[25] Q. Zhao(赵强)[1] Q. Z. Zhao(赵庆章)[9] S. J. Zhao(赵书俊)[46] T. C. Zhao(赵天池)[1]
Y. B. Zhao(赵豫斌)[1] Z. G. Zhao(赵政国)[40] A. Zhemchugov[19,a] B. Zheng(郑波)[41] J. P. Zheng(郑建平)[1]
Y. H. Zheng(郑阳恒)[36] B. Zhong(钟彬)[23] Z. Zhong(钟真)[9] L. Zhou(周莉)[1] X. K. Zhou(周晓康)[36]
X. R. Zhou(周小蓉)[40] C. Zhu(朱程)[1] K. Zhu(朱凯)[1] K. J. Zhu(朱科军)[1] S. H. Zhu(朱世海)[1]
X. L. Zhu(朱相雷)[33] Y. C. Zhu(朱莹春)[40] Y. M. Zhu(朱亚敏)[25] Y. S. Zhu(朱永生)[1] Z. A. Zhu(朱自安)[1]
J. Zhuang(庄建)[1] B. S. Zou(邹冰松)[1] J. H. Zou(邹佳恒)[1]
(BESIII Collaboration)

[1] Institute of High Energy Physics, Chinese Academy of Sciences Beijing 100049, China
[2] Bochum Ruhr-University, D-44780 Bochum, Germany
[3] Carnegie Mellon University, Pittsburgh, Pennsylvania 15213, USA
[4] Central China Normal University, Wuhan 430079, China
[5] China Center of Advanced Science and Technology, Beijing 100190, China
[6] G.I. Budker Institute of Nuclear Physics SB RAS (BINP), Novosibirsk 630090, Russia
[7] GSI Helmholtzcentre for Heavy Ion Research GmbH, D-64291 Darmstadt, Germany
[8] Guangxi Normal University, Guilin 541004, China
[9] GuangXi University, Nanning 530004, China
[10] Hangzhou Normal University, Hangzhou 310036, China
[11] Helmholtz Institute Mainz, Johann-Joachim-Becher-Weg 45, D-55099 Mainz, Germany
[12] Henan Normal University, Xinxiang 453007, China
[13] Henan University of Science and Technology, Luoyang 471003, China
[14] Huangshan College, Huangshan 245000, China
[15] Hunan University, Changsha 410082, China

[16] Indiana University, Bloomington, Indiana 47405, USA
[17] (A)INFN Laboratori Nazionali di Frascati, I-00044, Frascati, Italy; (B)INFN and University of Perugia, I-06100, Perugia, Italy
[18] Johannes Gutenberg University of Mainz, Johann-Joachim-Becher-Weg 45, D-55099 Mainz, Germany
[19] Joint Institute for Nuclear Research, 141980 Dubna, Moscow region, Russia
[20] KVI, University of Groningen, NL-9747 AA Groningen, The Netherlands
[21] Lanzhou University, Lanzhou 730000, China
[22] Liaoning University, Shenyang 110036, China
[23] Nanjing Normal University, Nanjing 210023, China
[24] Nanjing University, Nanjing 210093, China
[25] Nankai University, Tianjin 300071, China
[26] Peking University, Beijing 100871, China
[27] Seoul National University, Seoul, 151-747 Korea
[28] Shandong University, Jinan 250100, China
[29] Shanxi University, Taiyuan 030006, China
[30] Sichuan University, Chengdu 610064, China
[31] Soochow University, Suzhou 215006, China
[32] Sun Yat-Sen University, Guangzhou 510275, China
[33] Tsinghua University, Beijing 100084, China
[34] (A)Ankara University, Dogol Caddesi, 06100 Tandogan, Ankara, Turkey; (B)Dogus University, 34722 Istanbul, Turkey; (C)Uludag University, 16059 Bursa, Turkey
[35] Universitaet Giessen, D-35392 Giessen, Germany
[36] University of Chinese Academy of Sciences, Beijing 100049, China
[37] University of Hawaii, Honolulu, Hawaii 96822, USA
[38] University of Minnesota, Minneapolis, Minnesota 55455, USA
[39] University of Rochester, Rochester, New York 14627, USA
[40] University of Science and Technology of China, Hefei 230026, People's Republic of China
[41] University of South China, Hengyang 421001, China
[42] University of the Punjab, Lahore-54590, Pakistan
[43] (A)University of Turin, I-10125, Turin, Italy; (B)University of Eastern Piedmont, I-15121, Alessandria, Italy; (C)INFN, I-10125, Turin, Italy
[44] Wuhan University, Wuhan 430072, China
[45] Zhejiang University, Hangzhou 310027, China
[46] Zhengzhou University, Zhengzhou 450001, China
[a] Also at the Moscow Institute of Physics and Technology, Moscow 141700, Russia
[b] On leave from the Bogolyubov Institute for Theoretical Physics, Kiev 03680, Ukraine
[c] Also at the PNPI, Gatchina 188300, Russia
[d] Present address: Nagoya University, Nagoya 464-8601, Japan

Abstract: The number of ψ' events accumulated by the BESIII experiment from March 3 through April 14, 2009, is determined by counting inclusive hadronic events. The result is $106.41\times(1.00\pm0.81\%)\times10^6$. The error is systematic dominant; the statistical error is negligible.

Key words: ψ', inclusive, hadron, Bhabha

PACS: 13.25.Gv, 13.66.Bc, 13.20.Gd **DOI:** 10.1088/1674-1137/37/6/063001

1 Introduction

In 2009, the world's largest ψ' sample to date was collected at BESIII, allowing more extensive and precise studies of ψ' decays. The number of ψ' events, $N_{\psi'}$, is important in all ψ' analyses, including studies both of the direct decays of the ψ', as well as its daughters, χ_{cJ}, h_c, and η_c. The precision of $N_{\psi'}$ will directly affect the precision of all these measurements.

In this paper, we determine $N_{\psi'}$ with $\psi'\to$inclusive hadrons, whose branching ratio is known rather precisely, (97.85±0.13)% [1]. Also, a large off-resonance continuum data sample at $E_{\rm cm}=3.650$ GeV was collected. These events are very similar to the continuum background under the ψ' peak. Since the energy difference is very small, we can use the off-resonance data to estimate this background.

BEPC II is a double-ring e^+e^- collider designed to provide e^+e^- interactions with a peak luminosity of 10^{33} cm$^{-2}\cdot$s^{-1} at a beam current of 0.93 A. The cylindrical core of the BESIII detector consists of a helium-based main drift chamber (MDC), a plastic scintillator time-of-flight system (TOF), and a CsI(Tl) electromagnetic calorimeter (EMC), which are all enclosed in a superconducting solenoidal magnet providing a 1.0 T magnetic field. The solenoid is supported by an octagonal flux-return yoke with resistive plate counter muon identifier modules interleaved with steel. The acceptance for charged particles and photons is 93% over 4π stereo angle, and the charged-particle momentum and photon energy resolutions at 1 GeV are 0.5% and 2.5%, respectively.

The BESIII detector is modeled with a Monte Carlo (MC) simulation based on GEANT [2, 3]. For the simulation of inclusive ψ' decays, we use the EVTGEN generator [4]. Known ψ' decay channels are generated according to branching ratios in the PDG [1]; the remaining unknown decays are generated by the LUNDCHARM model [5]. An MC generated event is mixed with a random triggered event recorded in data taking to consider the possible background contamination such as beam-related background, cosmic rays, as well as the electronic noise and hot wires.

2 Event selection

There are many types of events in the data collected at the ψ' energy point, including $\psi' \to$ hadrons and lepton pairs (e^+e^-, $\mu^+\mu^-$, and $\tau^+\tau^-$), radiative returns to the J/ψ, and J/ψ decays from the extended tail of the J/ψ Breit-Wigner distribution. In addition, there are non-resonance (QED) processes, which make up the continuum background, including $e^+e^- \to \gamma^* \to$ hadrons, lepton pairs, and $e^+e^- \to e^+e^-$ +X (X=hadrons, lepton pairs). Non-collision events include cosmic rays, beam-associated background, and electronic noise. The signal channel is the process $\psi' \to$ hadrons. The data collected at the off-resonance energy include all of the above except ψ' decays.

Event selection includes track level selection and event level selection. At the track level, good charged tracks are required to pass within 1 cm of the beam line in the plane perpendicular to the beam and within $\pm$15 cm from the Interaction Point (IP) in the beam direction. Photon candidate showers reconstructed from the EMC barrel region ($|\cos\theta| < 0.8$) must have a minimum energy of 25 MeV, while those in the end-caps ($0.86 < |\cos\theta| < 0.92$) must have at least 50 MeV. The showers in the angular range between the barrel and end-cap are poorly reconstructed and excluded from the analysis. Requirements on the EMC cluster timing are applied to suppress electronic noise and energy deposits unrelated to the event.

At the event level, at least one good charged track is required. If the number of good charged tracks is larger than 2, i.e. $N_{\rm good} > 2$, no additional selection is needed. If $N_{\rm good} = 2$, where the Bhabha and dimuon events are dominant backgrounds, the momentum of each track is required to be less than 1.7 GeV/c, and the opening angle between the two tracks is required to be less than 176° to suppress these backgrounds. Figs. 1(a) and (b) show scatter plots of the momentum of one track versus that of another for MC simulated Bhabha events and inclusive MC events with two charged tracks, respectively. Figs. 2(a) and (b) show the opening angle distributions of MC simulated Bhabha events and inclusive MC events with two charged tracks, respectively. In addition, $E_{\rm visible}/E_{\rm cm} > 0.4$ is required to suppress low energy background (LEB), comprised mostly of $e^+e^- \to e^+e^-$+X and double ISR events ($e^+e^- \to \gamma_{\rm ISR}\gamma_{\rm ISR}$X). Here, $E_{\rm visible}$ denotes the visible energy which is defined as the energy sum of all charged tracks (calculated with the track momentum and assuming a $\pi^\pm$ mass) and neutral showers, and $E_{\rm cm}$ denotes the center-of-mass energy. Fig. 3(a) shows the $E_{\rm visible}$ distribution for data and inclusive MC events with two charged tracks. The excess in data at low energy is from the LEB.

If $N_{\rm good} = 1$, at least two additional photons are required in an event. From all photon pair combinations, the combination whose invariant mass, $M_{\gamma\gamma}$, is closest to the π^0 mass is selected, and $|M_{\gamma\gamma} - M_{\pi^0}| < 0.015$ GeV/c^2 is required. $E_{\rm visible}/E_{\rm cm} > 0.4$ is also required to suppress

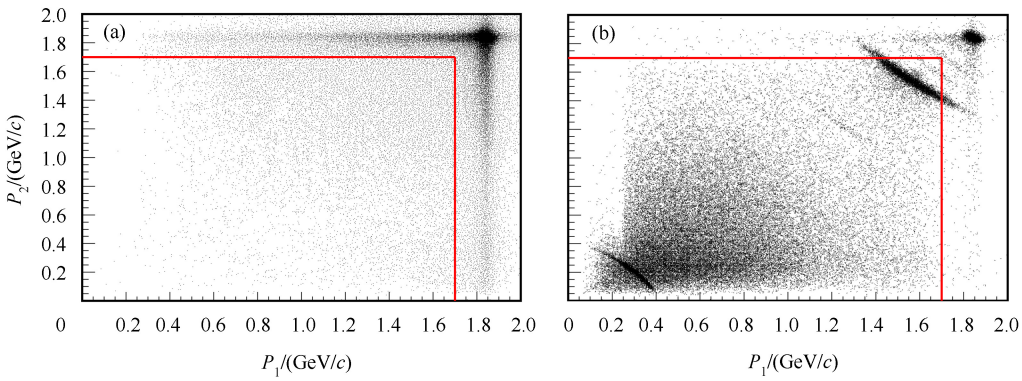


Fig. 1. The distribution of P_2 versus P_1. (a) For MC simulated Bhabha events, the horizontal and vertical lines show the selection requirements to remove Bhabha and $e^+e^- \to \mu^+\mu^-$ events; (b) For inclusive MC events with two charged tracks, the horizontal and vertical lines show the selection requirements to remove Bhabha and $e^+e^- \to \mu^+\mu^-$ events.

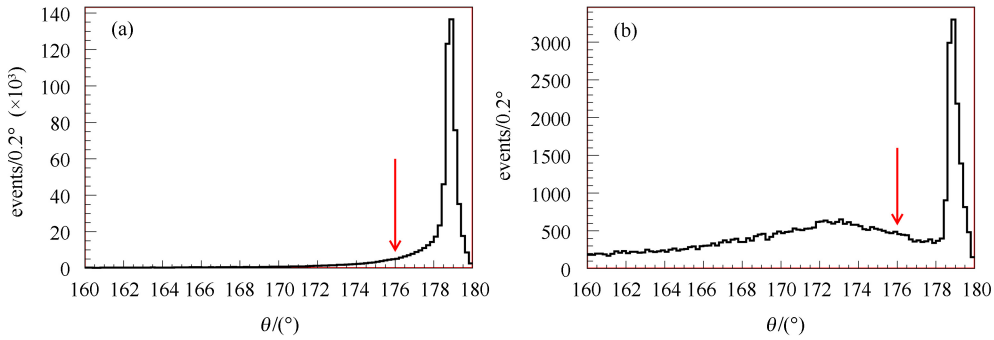


Fig. 2. The distribution of angle between tracks. (a) For MC simulated Bhabha events, the arrow shows the angle requirement used to remove most Bhabha events; (b) For inclusive MC events with two charged tracks, the arrow shows the angle requirement used to remove most Bhabha and $e^+e^-\to\mu^+\mu^-$ events.

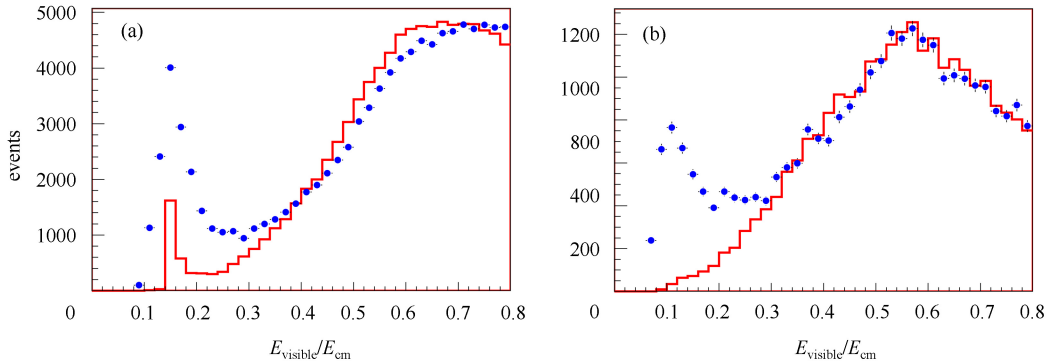


Fig. 3. The $E_{\rm visible}/E_{\rm cm}$ distribution normalized to $E_{\rm visible}/E_{\rm cm}>0.40$. Dots with error bars are data; the histogram is MC simulation (a) For $N_{\rm good}=2$ events; (b) For $N_{\rm good}=1$ events.

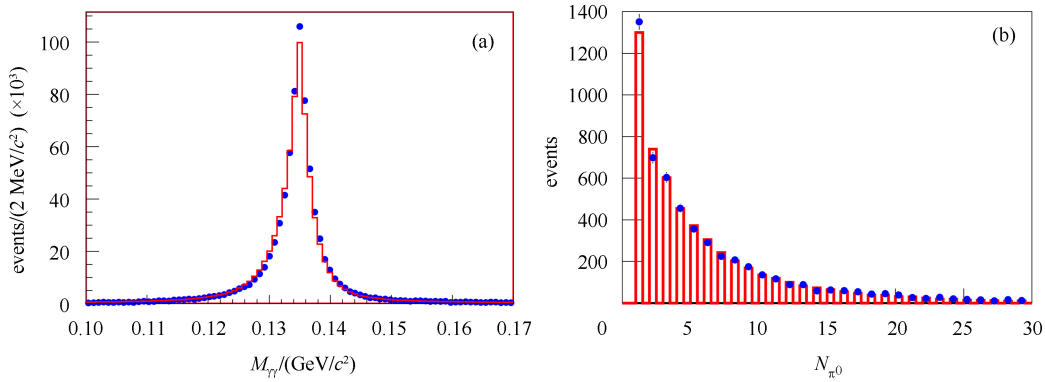


Fig. 4. (a) The $\gamma\gamma$ invariant mass ($M_{\gamma\gamma}$) distribution in the π^0 mass region for $N_{\rm good}=1$ events. The events in the region of 0.11 GeV/c^2 $<M_{\gamma\gamma}<$0.15 GeV/c^2 are taken as π^0 candidates; (b) The distribution of number of π^0 for $N_{\rm good}=1$ events. Dots with error bars are data while the histogram is MC simulation.

the LEB. Figs. 4(a), (b) show the $M_{\gamma\gamma}$ distributions in the π^0 mass region and number of π^0 candidates for data and MC simulation, respectively. In the comparison, QED background contribution has been subtracted from data. Fig. 3(b) shows the $E_{\rm visible}$ distribution for data and inclusive MC events. The excess in data at low energy is from LEB.

The average Z-direction vertex for an event is defined as

$$\bar{V}_Z=\frac{\sum_{i=1}^{N_{\rm good}}V_Z^i}{N_{\rm good}},$$

where V_Z is the distance along the beam direction of the

point of closest approach of a track to the IP. Fig. 5(a) shows the $\bar{V}_Z$ distribution for ψ' data after the above selection. Events satisfying $|\bar{V}_Z|<4.0$ cm are taken as signal, while events in the sideband region 6.0 cm$<|\bar{V}_Z|<$ 10.0 cm are taken as non-collision background events. The number of observed hadronic events ($N^{\rm obs.}$) is determined by

$$N^{\rm obs.}=N_{\rm signal}-N_{\rm sideband}. \quad (1)$$

Another method to determine the number of hadronic events (described below) is to fit the average Z-vertex with a double Gaussian to describe the signal and a polynomial to describe the non-collision events. This method is taken as cross check and to determine the systematic uncertainty.

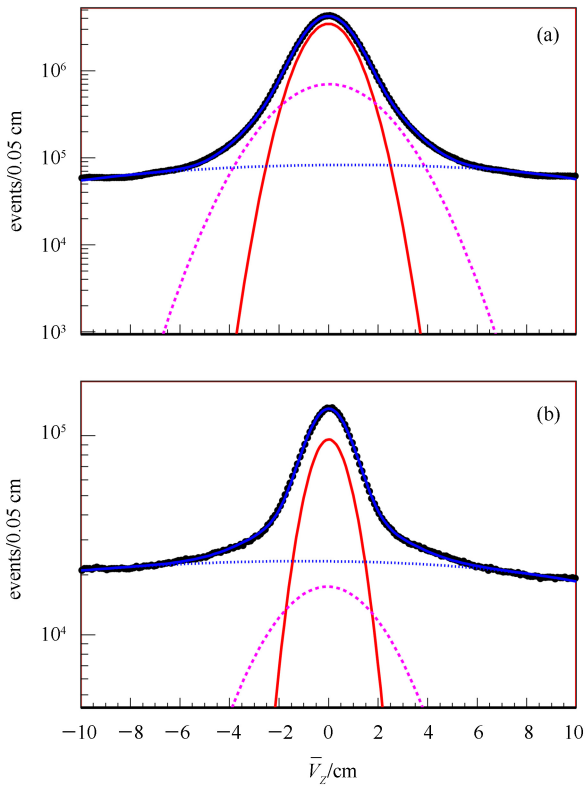


Fig. 5. The average Z vertex ($\bar{V}_Z$) distribution of hadronic events. The curves are a double Gaussian to describe the signal and a polynomial to describe the non-collision events. (a) For ψ' data; (b) For off-resonance data.

3 Background subtraction

In principle, the number of QED events can be estimated from:

$$N^{\rm QED}=\mathcal{L}\cdot\sigma\cdot\epsilon, \quad (2)$$

where $\mathcal{L}$ is the luminosity, and σ and ϵ are the cross-section and efficiency, respectively. σ is usually obtained from theoretical prediction, and ϵ is determined from MC simulation.

However in this analysis, we use the large sample of off-resonance data collected at 3.650 GeV to estimate the continuum background. The remained events, after imposing the same selection criteria in the off-resonance data, also form a peak in the $\bar{V}_Z$ distribution, as shown in Fig. 5(b). The same signal and sideband regions are used as for the ψ' data to determine the collision and non collision events. With this method, the continuum background subtraction is independent of MC simulation, and little systematic bias is introduced.

The contributions from radiative returns to J/ψ and J/ψ decays from the extended tail of the Breit-Wigner are very similar at the ψ' peak and off-resonance energy due to the small energy difference. They are estimated to be 1.11 and 1.03 nb at the ψ' peak and the off-resonance energy point, respectively, and according to MC simulation, the efficiencies for the known continuum processes at the two energy points are also similar. Therefore, the off-resonance data can be employed to subtract both the continuum QED and J/ψ decay backgrounds using a scaling factor, f, determined from the integrated luminosity multiplied by a factor of $1/s$ ($s=E_{\rm cm}^2$) to account for the energy dependence of the cross-section:

$$f=\frac{\mathcal{L}_{\psi'}}{\mathcal{L}_{3.650}}\cdot\frac{3.650^2}{3.686^2}=3.677, \quad (3)$$

where, $\mathcal{L}_{\psi'}$ and $\mathcal{L}_{3.650}$ are the integrated luminosities for ψ' data and 3.650 GeV data, respectively.

The luminosities at the two different energy points are determined from $e^+e^-\to\gamma\gamma$ events using the following track and event level selection criteria. At the track level, no good charged tracks and at least two showers are required. The energy for the most energetic shower should be higher than $0.7\times E_{\rm beam}$ while the second most energetic shower should be larger than $0.4\times E_{\rm beam}$, where $E_{\rm beam}$ is the beam energy. At the event level, the two most energetic showers in the ψ' rest frame should be back to back, and their phi angles must satisfy $178^\circ<|\phi_1-\phi_2|<182.0^\circ$. The luminosity systematic errors nearly cancel in calculating the scaling factor due to small energy difference between these two energy points. The f factor can also be obtained using luminosities determined with Bhabha events. It is found to be 3.685.

Also of concern is the LEB remaining in the ψ' events after the $E_{\rm visible}/E_{\rm cm}$ requirement. In order to test if the continuum background subtraction is also valid for these events, candidate LEB events are selected by requiring $E_{\rm visible}/E_{\rm cm}<0.35$ where there are few QED events expected. Figs. 6(a) and (b) show the comparison of $E_{\rm visible}/E_{\rm cm}$ between peak and off-resonance data for $N_{\rm good}=1$ and $N_{\rm good}=2$ events, respectively. The agreement between the two energy points is good for these events. The ratios of the numbers of peak and off-

resonance events for $N_{\rm good}=1$ and $N_{\rm good}=2$ are 3.3752 and 3.652, respectively. Compared with the scaling factor obtained from luminosity normalization in Eq. (3), a difference of about 10% is found for $N_{\rm good}=1$ while there is almost no difference for $N_{\rm good}=2$ events. These differences will be taken as systematic errors.

The small numbers of events from $\psi'\to e^+e^-$, $\mu^+\mu^-$, and $\tau^+\tau^-$ in data that pass our selection do not need to be explicitly subtracted since $\psi'\to$lepton events are included in the inclusive MC and those passing the selection criteria will contribute to the MC determined efficiency, so that their contribution cancels.

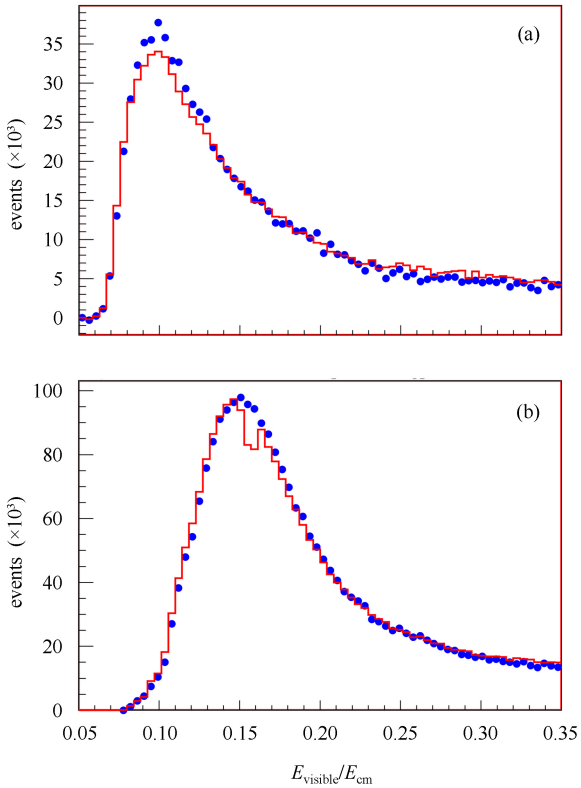


Fig. 6. Comparison of LEB events between ψ' peak and off-resonance data. Dots with error bars are ψ' data, and the histogram is off-resonance data. (a) For $N_{\rm good}=1$ events; (b) For $N_{\rm good}=2$ events.

Table 1 shows the number of observed hadronic events for different multiplicity requirements for ψ' and off-resonance data. Figs. 7, 8, and 9 show the cosθ, $E_{\rm visible}$, and charged-track multiplicity distributions after subtracting all backgrounds. In the comparison, QED background contribution has been subtracted from data.

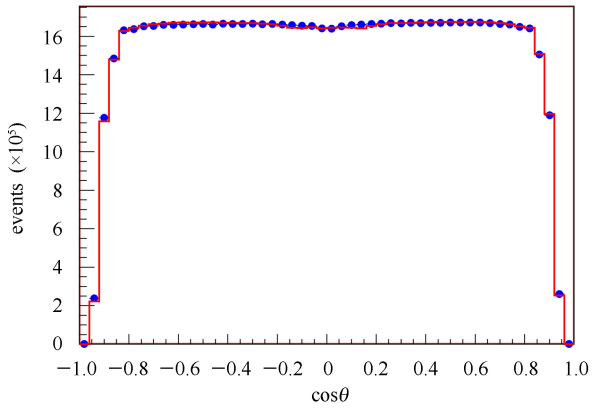


Fig. 7. The cosθ distribution for charged tracks. Dots with error bars are data; the histogram is MC simulation.

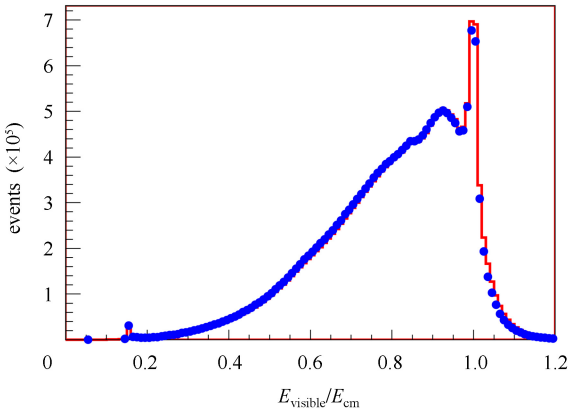


Fig. 8. The visible energy distribution. Dots with error bars are data; the histogram is MC simulation.

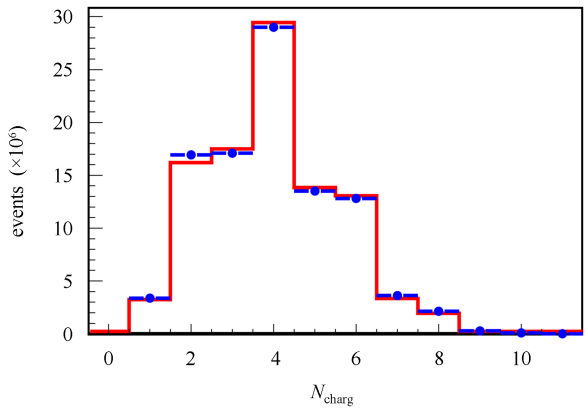


Fig. 9. The charged-track multiplicity distribution. Dots with error bars are data; the histogram is MC simulation.

Table 1. $N^{\rm obs.}$ for peak and off-resonance data ($\times10^6$), and the detection efficiency for inclusive ψ' decay events determined with 106×10^6 $\psi'\to$ inclusive MC events.

	$N_{\rm good}\geqslant1$	$N_{\rm good}\geqslant2$	$N_{\rm good}\geqslant3$	$N_{\rm good}\geqslant4$
ψ' data	106.928	102.791	81.158	63.063
off-resonance data	2.192	1.98	0.704	0.433
ϵ(%)	92.912	89.860	74.624	58.188

4 Numerical result

The number of ψ' events is determined from

$$N_{\psi'}=\frac{N^{\rm obs.}_{\rm peak}-f\cdot N^{\rm obs.}_{\rm off-resonance}}{\epsilon}, \quad (4)$$

where, $N^{\rm obs.}_{\rm peak}$ is the number of hadronic events observed at the ψ' peak from Eq. (1), $N^{\rm obs.}_{\rm off-resonance}$ is the number of hadronic events observed at the off-resonance energy point, $E_{\rm cm}=3.650$ GeV, with the same selection criteria as those for peak data, and ϵ is the selection efficiency obtained from the inclusive ψ' MC sample, the branching fraction of $\psi'\to$ inclusive hadron is included in the efficiency. The relevant numbers are listed in Table 1 for different $N_{\rm good}$ selection requirements. The factor f is the scaling factor which has been introduced in Eq. (3). With these numbers, we obtain the numerical result for $N_{\psi'}$ listed in Table 2 for different choices of $N_{\rm good}$. We take the result for $N_{\rm good}\geqslant1$ as the central value of our final result.

Table 2. $N_{\psi'}$ ($\times10^6$) for different charged-track multiplicity requirements.

	$N_{\rm good}\geq1$	$N_{\rm good}\geqslant2$	$N_{\rm good}\geqslant3$	$N_{\rm good}\geqslant4$
$N_{\psi'}$	106.414	106.279	105.289	105.643

5 Systematic uncertainties

The systematic uncertainties include the uncertainties caused by tracking, the event start time (T_0), trigger efficiency, background contamination, the selection of the signal and sideband regions, etc.

5.1 Tracking

Generally, the tracking efficiency for MC events is higher than that of data according to various studies [6]. Assuming the average efficiency difference between data and MC is 1% per track, the effect can be measured by randomly tossing out 1% of MC simulated tracks. Only a difference of 0.03% on $N_{\psi'}$ is found for $N_{\rm good}\geqslant1$ events with and without this tracking efficiency change; $N_{\psi'}$ is not sensitive to the tracking efficiency.

5.2 Charged-track multiplicity

Figure 9 shows that the MC does not simulate the charged-track multiplicity very well. The uncertainty due to charged-track multiplicity simulation can be estimated by an unfolding method, which is described as follows. The generated true charged multiplicity in MC simulation is even, i.e., 0, 2, 4, 6, 8, ···. The observed MC multiplicity distribution is obtained after simulation and event selection. For example, if the generated true multiplicity is 4, the observed multiplicities are 0, 1, 2, 3, 4 or higher with different probabilities. Therefore, an efficiency matrix, ϵ_{ij}, which describes the efficiency of an event generated with j charged tracks to be reconstructed with i charged tracks, is obtained from MC simulation. The distribution of the number of observed charged-track events in data, $N_i^{\rm obs.}$, is known. The true multiplicity distribution in data can be estimated from the observed multiplicity distribution in data and the efficiency matrix by minimizing the χ^2. The χ^2 is defined as

$$\chi^2=\sum_{i=1}^{10}\frac{\left(N_i^{\rm obs.}-\sum\limits_{j=0}^{10}\epsilon_{ij}\cdot N_j\right)^2}{N_i^{\rm obs.}}, \quad (5)$$

where the N_j ($j=0,\ 2,\ 4,\ 6,\ 8,\ 10$) describe the true multiplicity distribution in data and are taken as floating parameters in the fit. The simulation is only done up to a true multiplicity of 10, since there are few events at high multiplicity. The total true number of events in data can be obtained by summing all fitted N_j; it is 105.96×10^6 which is lower than the nominal value by 0.4%. We take this difference as the uncertainty due to the charged-track multiplicity distribution.

5.3 Momentum and opening angle

For $N_{\rm good}=2$ events, momentum and opening angle requirements are used to remove the huge number of Bhabha events. When the momentum requirement is changed from $P<1.7$ GeV/c to $P<1.55$ GeV/c, the corresponding $N^{\rm obs.}$ for peak and off-resonance data, as well as the efficiency change, but the change in $N_{\psi'}$ is only 0.05%. When the angle requirement is changed from $\theta<176^\circ$ to $\theta<160^\circ$, the change in $N_{\psi'}$ is 0.01%. Therefore, the total uncertainty due to momentum and opening angle requirements is 0.05%. Figs. 10(a) and (b) show comparisons between data and MC simulations for momentum and opening angle distributions after subtracting backgrounds, respectively. In the comparison, QED background contribution has been subtracted from data.

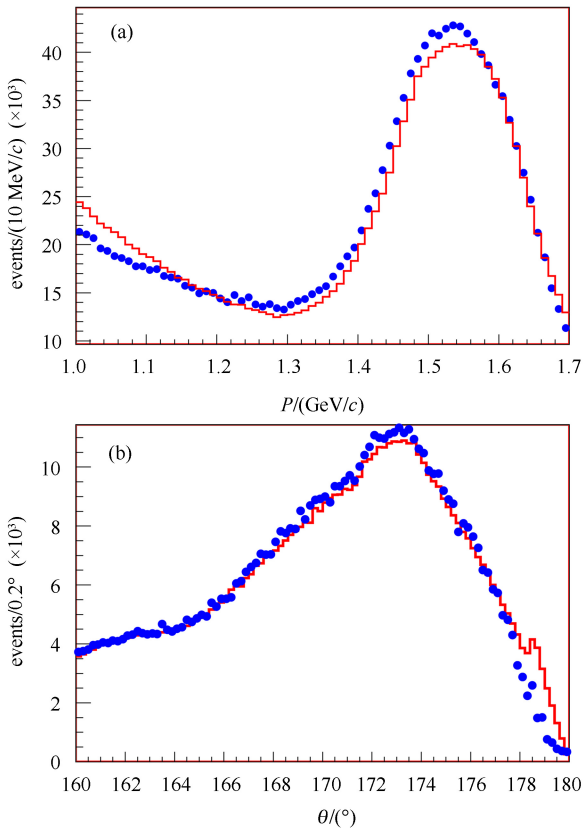


Fig. 10. The distribution of total momentum (a) and opening angle between tracks (b) for $N_{\rm good}=2$ events. Dots with error bars are data; the histogram is MC simulation.

5.4 LEB background contamination

$N_{\psi'}$ is insensitive to the visible energy requirement. The difference between a tight requirement, $E_{\rm visible}/E_{\rm cm}>0.45$, and no requirement is only 0.1%. Conservatively, an uncertainty of 0.1% is assigned due to the background contamination.

5.5 Determination of number of hadronic events

Two methods are used to obtain $N^{\rm obs.}$. The first is to directly count the numbers of events in the signal and sideband regions; the second method is to fit the $\bar{V}_Z$ distribution with a double Gaussian for the signal and a polynomial for the background, as shown in Figs. 5(a) and (b). A difference of 0.28% is found between these two methods which is taken as the uncertainty due to the $N^{\rm obs.}$ determination.

5.6 Vertex limit

When $V_{\rm r}<1$ cm is changed to $V_{\rm r}<2$ cm, $N_{\psi'}$ changes by 0.35%, while if $|\bar{V}_Z|<10$ cm is changed to $|\bar{V}_Z|<15$ cm, there is almost no change. Therefore, the difference of 0.35% is taken as the uncertainty from the vertex requirement.

5.7 Scaling factor

The scaling factor can be obtained for two different QED processes, $e^+e^-\to\gamma\gamma$ and $e^+e^-\to e^+e^-$. The corresponding results are 3.677 and 3.685. The difference on $N_{\psi'}$ due to the f factor can be calculated by $\Delta f\cdot N^{\rm obs.}_{N_{\rm good}\geqslant1}(3.650\ {\rm GeV})/N_{\psi'}=(3.685\text{–}3.677)\cdot2.192/106.41=0.016\%$, where $2.192(\times10^6)$ is the number of selected events for $N_{\rm good}\geqslant1$ in off-resonance data (see Table 1), and 106.41 $(\times10^6)$ is the measured total number of ψ'. This difference is taken as a systematic uncertainty.

5.8 Choice of sideband region

We take $|\bar{V}_Z|<4.0$ cm as the signal region and $6<|\bar{V}_Z|<10$ cm as the sideband region. A difference of 0.45% in $N_{\psi'}$ is found by shifting the sideband region outward by 1.0 cm, which is about 1σ of the $\bar{V}_Z$ resolution, i.e., the sideband region is changed from 6 cm$<|\bar{V}_Z|<$10 cm to 7 cm$<|\bar{V}_Z|<$11 cm. We take this difference as the uncertainty caused by choice of the sideband region.

5.9 π^0 mass requirement

This requirement is only used for $N_{\rm good}=1$ events. $N_{\psi'}$ has a slight change of 0.11% when the mass window requirement is changed from $|M_{\gamma\gamma}-M_{\pi^0}|<0.015\ {\rm GeV}/c^2$ to $|M_{\gamma\gamma}-M_{\pi^0}|<0.025\ {\rm GeV}/c^2$; this difference is taken as the uncertainty due to π^0 mass requirement.

5.10 The cross section of $e^+e^-\to\tau^+\tau^-$

Since the off-resonance energy point is not very far from $\tau\tau$ threshold, $\sigma(e^+e^-\to\tau^+\tau^-)$ does not vary as $1/s$ between the off-resonance energy and the ψ' peak, as other QED processes. The difference between the observed and the cross section assuming a $1/s$ dependence causes a change of 0.17% in $N_{\psi'}$. This change is taken as a systematic uncertainty.

5.11 B($\psi'\to$X+J/ψ)

The ψ' MC assumes $B(\psi'\to X+J/\psi)\approx57\%$ from the PDG [1], while the CLEO experiment determined a branching ratio of 62% [7]. Using CLEO's result, a new inclusive MC sample was generated. The corresponding efficiencies are 92.912%, 89.761%, 74.838% and 58.528% for $N_{\rm good}\geqslant1$, 2, 3 and 4, respectively. Compared with numbers in Table 1, the efficiency differences between these two MC samples are negligible.

5.12 Event start time determination

The Event Start Time (EST) algorithm is used to determine the common start time of the recorded tracks in an event. The efficiency of the EST determination affects the resolution of tracks from the tracking algorithm. These efficiencies for different charged tracks, e, μ, π, K, and p, and photons are studied with different control

samples for both data and inclusive MC events, for example, $J/\psi \to \pi^+\pi^-\pi^0$, $\pi^+\pi^-p\bar{p}$, and $\psi' \to \pi^+\pi^- J/\psi$, $J/\psi \to l^+l^-$, etc. All comparisons indicate that the efficiencies of the EST determination are high for both track and event level ($>98\%$) selection, and the difference between data and MC simulated events is quite small ($\sim 0.1\%$). We take this difference as the uncertainty caused by the EST determination.

5.13 Trigger efficiency

The fraction of events with $N_{\rm ngood} \geqslant 2$ is about 97%. The trigger efficiency for these events is close to 100.0% according to a study of the trigger efficiency [8]. For $N_{\rm good}=1$ events, an extra π^0 is required, and the hadron trigger efficiency for this channel is 98.7% [8]. Since the fraction of $N_{\rm good}=1$ events is only about 3%, the uncertainty caused by the trigger is negligible.

5.14 The missing 0-prong hadronic events

A detailed topology analysis is performed for $N_{\rm good}=0$ events in the inclusive MC sample. Most of these events come from known decay channels, such as $\psi' \to X + J/\psi$ ($X = \eta$, $\pi^0\pi^0$, and $\pi^+\pi^-$), $\psi' \to \gamma\chi_{cJ}$, and $\psi' \to e^+e^-$, $\mu^+\mu^-$. The fraction of pure neutral events is less than 1.0%. For the known charged decay modes, the MC simulation works well according to many comparisons between data and MC simulation in Section 3. To investigate the pure neutral channels, the same selection criteria at the track level are used. The criteria at the event level include $N_{\rm good}=0$ and $N_\gamma>3$. The latter requirement is used to suppress $e^+e^- \to \gamma\gamma$ and beam-associated background events. The same selection criteria are imposed on the off-resonance data. Figs. 11(a) and (b) show the distribution of total energy in the EMC for data and inclusive MC events. The peaking events correspond to the pure neutral candidates, and the number of events is extracted by fitting. The difference in the number of fitted events between data and inclusive MC events is found to be 17%. Therefore, the uncertainty due to the pure neutral events should be less than $17\% \times 1\% = 0.17\%$, and this is taken as the systematic uncertainty on the missing 0-prong events.

5.15 B($\psi' \to$hadrons)

The uncertainty of B($\psi' \to$hadrons) is very small according to the PDG [1], 0.13%, which is taken as the uncertainty due to ψ' decays to hadronic events.

5.16 MC modeling

The uncertainty due to simulation of ψ' inclusive decays arises from the input of branching ratios, the angular distribution of known decay modes, how to fill the unknown decay modes, etc. The uncertainties caused by branching ratios $\psi' \to X+J/\psi$ and $\psi' \to$hadrons have

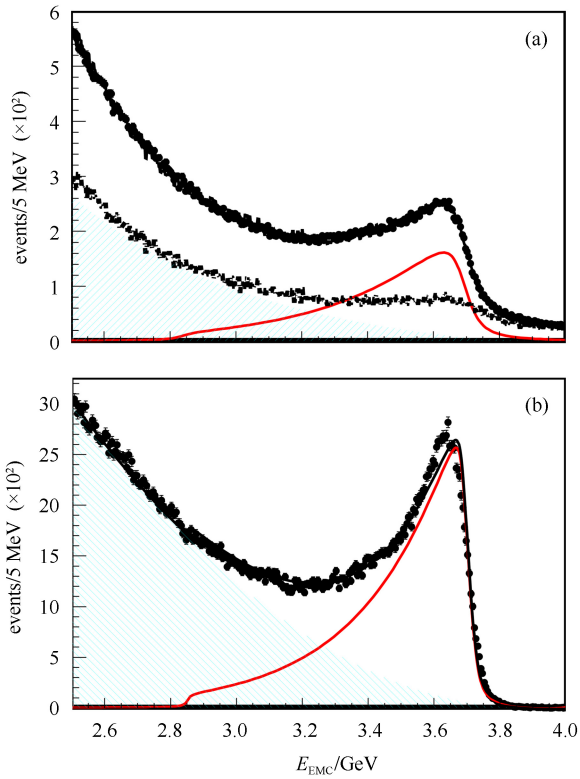


Fig. 11. The distribution of total energy in the EMC with $N_{\rm good}=0$ The dot-dashed line denotes the signal shape of $\psi' \to$neutral channel, and the shaded region is the background shape from ψ' decay. (a) For ψ' data, the dashed line denotes the background shape from QED processes. (b) For inclusive MC events.

Table 3. The systematic uncertainty (%)

source	uncertainty
background contamination	0.10
$N^{\rm obs.}$ determination	0.28
choice of sideband region	0.45
vertex selection	0.35
momentum and opening angle	0.05
scaling factor (f)	0.02
0-prong events	0.17
tracking	0.03
charged-track multiplicity	0.40
$\sigma(e^+e^- \to \tau^+\tau^-)$	0.17
B($\psi' \to X+J/\psi$)	0.00
π^0 mass requirement	0.11
EST determination	0.10
trigger efficiency	negligible
B($\psi' \to$hadron)	0.13
total	0.81

been estimated. The possible imperfection from other MC modeling, in fact, can be reflected by tracking, charged-track multiplicity, and the missing of 0-prong events. The uncertainties caused by above sources have also been studied carefully. Therefore, it is not necessary to introduce an extra uncertainty due to MC modeling.

5.17 Total uncertainty

Table 3 lists all systematic errors. The total systematic uncertainty is determined by the quadratic sum of all uncertainties.

6 Summary

The number of ψ' events is determined using $\psi' \to$ hadrons. The large off-resonance data sample at $E_{\rm cm}$=3.650 GeV is used to estimate the background under the ψ' peak. The number of ψ' events taken in 2009 is measured to be $(106.41 \pm 0.86) \times 10^6$, where the error is systematic dominant and the statistical error is negligible.

The BESIII collaboration thanks the staff of BEPCII and the computing center for their hard efforts.

References

1 Beringer J et al. (Particle Data Group). Phys. Rev. D, 2012, **86**: 010001
2 Agostinelli S et al. (GEANT4 Collaboration). Nucl. Instrum. Methods A, 2003, **506**: 250
3 Allison J et al. IEEE Trans. Nucl. Sci., 2006, **53**: 270
4 PING R G et al. Chinese Physics C (HEP & NP), 2008, **32**: 599
5 CHEN J C et al. Phys. Rev. D, 2005, **70**: 011102(R)
6 Ablikim M et al. (BESIII collaboration). Phys. Lett. B, 2012, **710**: 594
7 Mendez H et al. (CLEO collaboration). Phys. Rev. D, 2008, **78**: 011102(R)
8 Berger N et al. Chinese Physics C (HEP & NP), 2010, **34**: 1779